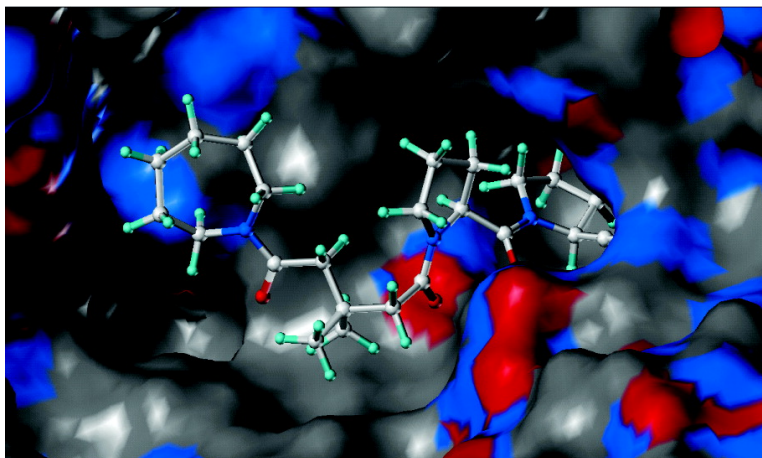


Dicarboxylic Acid Azacycle I-Prolyl-pyrrolidine Amides as Prolyl Oligopeptidase Inhibitors and Three-Dimensional Quantitative Structure–Activity Relationship of the Enzyme–Inhibitor Interactions

Elina M. Jarho, Erik A. A. Walln, Johannes A. M. Christiaans, Markus M. Forsberg, Jarkko I. Venlinen, Pekka T. Mnnist, Jukka Gynther, and Antti Poso

J. Med. Chem., **2005**, 48 (15), 4772-4782 • DOI: 10.1021/jm0500020 • Publication Date (Web): 25 June 2005

Downloaded from <http://pubs.acs.org> on March 28, 2009



More About This Article

Additional resources and features associated with this article are available within the HTML version:

- Supporting Information
- Links to the 3 articles that cite this article, as of the time of this article download
- Access to high resolution figures
- Links to articles and content related to this article
- Copyright permission to reproduce figures and/or text from this article

[View the Full Text HTML](#)

Dicarboxylic Acid Azacycle L-Prolyl-pyrrolidine Amides as Prolyl Oligopeptidase Inhibitors and Three-Dimensional Quantitative Structure–Activity Relationship of the Enzyme–Inhibitor Interactions

Elina M. Jarho,^{*,†} Erik A. A. Wallén,[†] Johannes A. M. Christiaans,^{†,‡} Markus M. Forsberg,[§] Jarkko I. Venäläinen,[§] Pekka T. Männistö,^{§,||} Jukka Gynther,[†] and Antti Poso[†]

Departments of Pharmaceutical Chemistry and Pharmacology and Toxicology, P.O. Box 1627, FI-70211 Kuopio, Finland

Received January 3, 2005

A series of dicarboxylic acid azacycle L-prolyl-pyrrolidine amides was synthesized, and their inhibitory activity against prolyl oligopeptidase (POP) from porcine brain was tested. Three different azacycles were tested at the position beyond P3 and six different dicarboxylic acids at the P3 position. L-Prolyl-pyrrolidine and L-prolyl-2(S)-cyanopyrrolidine were used at the P2–P1 positions. The IC₅₀ values ranged from 0.39 to 19000 nM. The most potent inhibitor was the 3,3-dimethylglutaric acid azepane L-prolyl-2(S)-cyanopyrrolidine amide. Molecular docking (GOLD) was used to analyze binding interactions between different POP inhibitors of this type and the POP enzyme. The data set consisted of the novel inhibitors, inhibitors published previously by our group, and well-known reference compounds. The alignments were further analyzed using comparative molecular similarity indices analysis. The binding of the inhibitors was consistent at the P1–P3 positions. Beyond the P3 position, two different binding modes were found, one that favors lipophilic structures and one that favors nonhydrophobic structures.

Introduction

Prolyl oligopeptidase (POP, EC 3.4.21.26) is a member of the POP family of serine proteases.¹ It is a large, 80 kDa enzyme with both a cytosolic and a particulate form.^{2,3} POP hydrolyzes oligopeptides at the carboxyl side of a proline residue, with the exception of an amide bond between two proline residues and the first two amide bonds at the amino terminus.⁴

POP has been related to cognitive disorders because several substrates of POP, like substance P,⁵ vasopressin,^{6–8} and thyroliberin,⁹ have memory-promoting effects. In addition, substance P has been reported to prevent the neurotoxic effects of the amyloid β peptide, often deposited in the brains of Alzheimer patients.¹⁰ In the human brain, the highest POP activity has been found in the cortex.^{11,12} POP coexists with several neuropeptide receptors, and it is possibly involved in inactivation of regulatory neuropeptides.¹³ Exceptionally high POP gene transcriptions have been found in the hypothalamus and cortex of aged mice,¹⁴ and on the other hand, a stimulating environment has been shown to decrease POP gene expression in the cortex of mice.¹⁵ The inhibition of POP has been shown to prevent scopolamine-, ischemia-, and lesion-induced amnesia in rats.^{16–18} Furthermore, the inhibition of POP has been shown to enhance cognition in a model of early Parkinsonism in monkeys.¹⁹

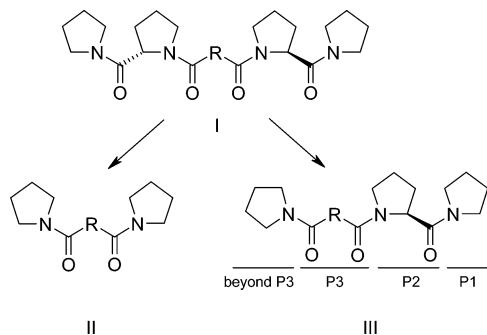


Figure 1. Rationale behind the novel inhibitors. (I) A series of large symmetrical POP inhibitors.²¹ (II) A series of small symmetrical compounds, which were very poor POP inhibitors. (III) A series of the novel POP inhibitors.

Recently, the POP of *Trypanosoma cruzi* has also been implicated as a therapeutic target. *T. cruzi* causes Chagas' disease, and the parasitic POP is presumably involved in the invasion of host cells. Selective inhibitors of the parasitic POP prevented the invasion.²⁰

Our group published recently a series of large, symmetrical POP inhibitors (I in Figure 1).²¹ These inhibitors were very potent, and another series of large inhibitors were developed from the first set of compounds.²² To diversify the compound set for the three-dimensional (3D) quantitative structure–activity relationship (QSAR) study, two series of smaller compounds were synthesized. The removal of the pyrrolidine-1-carbonyl group from both ends (II in Figure 1, not published) decreased strongly the potency. The succinic acid dipyrrolidine amide was the only compound with a weak inhibitory activity. (It had an IC₅₀ value of 13 μ M against POP from rat brain. Inhibitory activities against POP from rat brain and porcine brain are

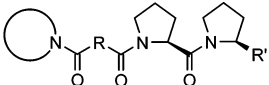
* To whom correspondence should be addressed. Tel: +358-17-162460. Fax: +358-17-162456. E-mail: Elina.Jarho@uku.fi.

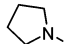
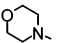
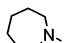
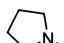
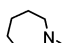
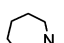
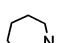
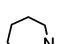
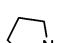
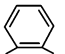
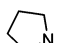
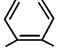
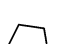
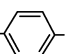
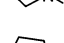
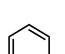
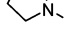
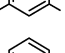
[†] Department of Pharmaceutical Chemistry.

[‡] Present address: Altana Pharma bv, P.O. Box 31, 2130 AA Hoofddorp, The Netherlands.

[§] Department of Pharmacology and Toxicology.

^{||} Present address: Division of Pharmacology and Toxicology, Faculty of Pharmacy, P.O. Box 56, FI-00014 University of Helsinki, Finland.

Table 1. Structures and Inhibitory Activities (95% Confidence Intervals Are Presented in Parentheses) of the Synthesized Compounds


Compound	R	R'	IC ₅₀ (nM) ^a
3		-CH ₂ -CH ₂ -	110 (110 – 120)
4		-CH ₂ -CH ₂ -	1200 (940 – 1400)
5		-CH ₂ -CH ₂ -	41 (35 – 48)
11		-CH ₂ -CH ₂ -	2.9 (1.9 – 4.4)
12		-CH ₂ -CH ₂ -	0.76 (0.50 – 1.2)
13		-CH ₂ -CH ₂ -CH ₂ -	28 (17 – 44)
14		-CH ₂ -CH ₂ -CH ₂ -	1.2 (0.70 – 2.0)
15		-CH ₂ -C(CH ₃) ₂ -CH ₂ -	0.39 (0.27 – 0.56)
16			19000 (14000 – 27000)
17			1500 (1300 – 1700)
18			1.6 (1.3 – 2.0)
19			6.9 (6.2 – 7.8)
20			4.6 (3.4 – 6.2)

^a The IC₅₀ values were determined against POP from porcine brain as described in the Experimental Section.

similar in our test system.) These compounds were not included in the 3D QSAR study. Removal of the pyrrolidine-1-carbonyl group from only one end, however, resulted in a new series of potent inhibitors, most of them having the IC₅₀ value in the nanomolar range (III in Figure 1).

The 3D QSAR models were created using the comparative molecular similarity indices analysis (CoMSIA) method, which produces information of the favored and disfavored properties of the examined compound set.²³ The compound set consisted of the novel inhibitors published in this article (Table 1) and the previously published inhibitors and reference compounds (Table 2). These data are useful to explain and predict activities of different POP inhibitors and to find out how different types of POP inhibitors may bind to the active site of the enzyme. To our knowledge, this is the first time when the systematic molecular docking and 3D QSAR studies have been described for POP inhibitors.

Methods

Synthetic Chemistry. A series of dicarboxylic acid azacycle L-prolyl-pyrrolidine amides was synthesized (Table 1). L-Pro-pyrrolidine and L-Pro-2(*S*)-cyano-pyrrolidine were used at the P2–P1 positions, and

different dicarboxylic acids coupled to different azacycles were used at the positions P3 and beyond P3. The inhibitors were synthesized via the synthetic routes described in Schemes 1 and 2 using a similar set of chemical reactions. The building blocks were coupled to each other by amide bonds, which were synthesized in two different ways: The carboxylic acid was activated with pivaloyl chloride and reacted with the amine, or the dicarboxylic anhydride was reacted with the amine. The only problematic step was the deprotection of BOC-2(*S*)-cyanopyrrolidine. The cyano group reacted to some extent during the deprotection, and consequently, the yields of these coupling reactions were low, ranging from 10 to 45% for compounds **11**, **12**, **17**, **19**, and **20**. Therefore, the cyano group was introduced in the last synthetic step of the compounds that were made in the later part of the study (**14**, **15**, and **18**). The compounds in Table 2 were synthesized as described previously.^{21,22,24–26}

Molecular Modeling. The structure of POP, 1QFS (native),²⁷ was derived from PDB and the cocrystallized inhibitor (*Z*-L-Pro-L-prolinal) was removed from the crystal structure. The POP inhibitors in Table 1 and the previously published compounds in Table 2 were docked into this crystal structure of POP using the GOLD program.²⁸ The docking area was defined using the NE atom of ARG643 as a center, with a radius of 20 Å. Unfortunately, current docking programs cannot automatically take into account a possible covalent interaction between a ligand and a host. Because several of the compounds possibly have a covalent interaction, two violations for steric clashes were allowed. With these settings, all of the compounds were docked successfully into the active site of POP.

The dockings were further analyzed using the CoMSIA method,²³ and a statistically valid 3D QSAR model was created. Originally, CoMSIA was carried out by using all five different field types, namely, steric, electrostatic, hydrophobic, acceptor, and donor fields. Even this model was statistically valid (q^2 close to 0.7 with six components). However, a closer inspection revealed that most of the model was explained by the acceptor, electrostatic, and hydrophobic fields, which were then used in the final models. The selection of the partial least squares (PLS) components was based on Scrambling stability test, as proposed by Clark and Fox.²⁹ This test yields adapted q^2 , CSDEP and $dq^{**2}/dr2yy$ values. CSDEP had the optimum with three PLS components and the $dq^{**2}/dr2yy$ well below 1 (0.91), indicating low enough PLS component number. The final CoMSIA model had the following leave-one-out PLS statistics: $q^2 = 0.69$, $S_{PRESS} = 0.65$, three PLS components. The final nonvalidated model resulted in $r^2 = 0.91$, F value = 175, and s value = 0.34.

Results and Discussion

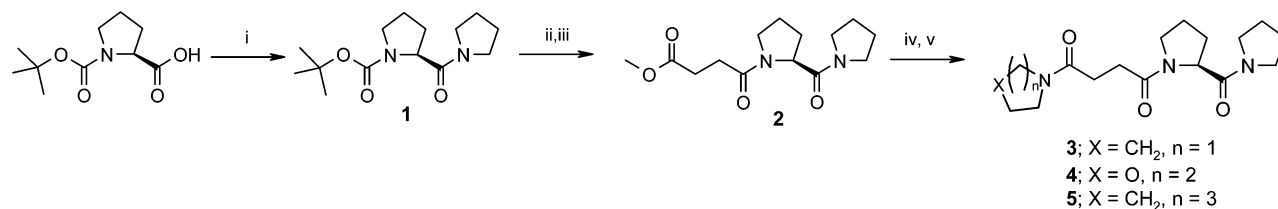
Molecular Docking. All compounds were successfully docked into the binding cavity of POP. When selected dockings are analyzed together, it is obvious that most of the compounds occupy in general the same binding area. Because GOLD produces usually several alternative binding modes, other binding modes were also detected, but in all cases, the selection was based on the scoring function of GOLD. The only exception

Table 2. Structures and Inhibitory Activities of the Previously Published Compounds and the Reference Compounds

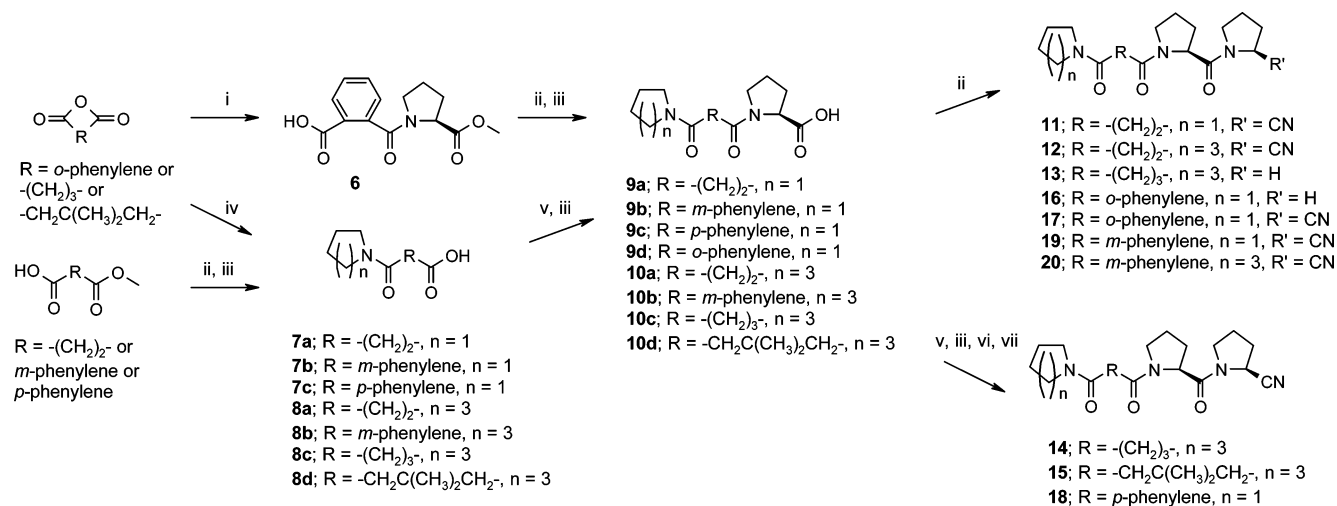
compd	structure	IC ₅₀ (nM) ^a	ref
21		77	21
22		48	21
23		13	21
24		0.57	22
25		0.32	22
26		68	21
27		81	21
28		26	21
29		31	22
30		23	22
31		33	22
32		170	22
33		14	22
34		65	22
35		78	22
36		18	22
37		1.5	21
38		1.1	22
39		0.72	22
40		4.2	22

compd	structure	IC ₅₀ (nM) ^a	ref
41		1.6	22
42		1.3	22
43		1.3	21
44		0.39	21
45		0.61	22
46		1.2	22
47		640	22
48		87	22
49		81	22
50		110	22
51		39	22
52		66	21,30
53		29	24,31
54 ^b		3.1	-
55		2.2	21,32
SUAM-1221			
56		0.22	26
57		0.22	25
58		0.20	25,33
JTP-4819			
59		0.33	21,34
Z-Pro-prolinal			

^a The IC₅₀ values were determined against POP from porcine brain as described in the Experimental Section. ^b Not published before.

Scheme 1^a

^a Reagents and conditions: (i) 1. Et₃N, pivaloyl chloride/dichloromethane, 0 °C; 2. Et₃N, pyrrolidine/dichloromethane. (ii) HCl/EtOAc. (iii) Succinic acid monomethyl ester pivalic acid anhydride (prepared from succinic acid monomethyl ester and pivaloyl chloride in dichloromethane at 0 °C), Et₃N/dichloromethane. (iv) LiOH/MeOH–H₂O. (v) 1. Et₃N, pivaloyl chloride/dichloromethane, 0 °C; 2. Et₃N, pyrrolidine or morpholine, or azepane/dichloromethane.

Scheme 2^a

^a Reagents and conditions: (i) L-Proline methyl ester HCl salt, Et₃N/dichloromethane. (ii) 1. Et₃N, pivaloyl chloride/dichloromethane, 0 °C; 2. Et₃N, pyrrolidine or azepane, or 2(*S*)-cyanopyrrolidine/dichloromethane. (iii) LiOH/MeOH–H₂O. (iv) Azepane/THF. (v) 1. Et₃N, pivaloyl chloride/dichloromethane, 0 °C; 2. Et₃N, L-proline methyl ester HCl salt/dichloromethane. (vi) 1. Et₃N, ethyl chloroformate/THF, –10 °C; 2. NH₃/H₂O. (vii) Et₃N, trifluoroacetic anhydride/THF, 0 °C.

was compound **32**, where the GOLD-proposed docking was replaced by the CSCORE-proposed docking. The binding mode that GOLD proposed to be the best for compound **32** differed in the P1–P2 area from the rest of the compounds. To obtain a better mode, a CSCORE calculation within Sybyl was carried out.

The data set consisted of POP inhibitors with varying inhibitory activities. There was not much structural variation at the P1 and P2 positions and without exception, these positions were bound as in the original crystal structure.²⁷ Most of the variation was at the P3 position and beyond it. However, there is a S3 binding site for the P3 position, which is occupied by all ligands. This position is surrounded by the lipophilic residues ILE591, ALA594, CYS259, and PHE173. Beyond the P3 position, conformational freedom increases and one consistent binding site was not found. Instead, two binding modes, which are clearly favored, were found. Each of them is represented by one inhibitor in Figure 2a. The more populated binding mode is called binding mode A (compound **15** in Figure 2a). It is occupied by 60% of the ligands, and it is surrounded by GLY254, CYS255, ARG252, and MET245. The less populated binding mode is called binding mode B (compound **14** in Figure 2a), and it is occupied by 40% of the ligands. Both binding modes resulted in equal inhibitory activities.

The novel inhibitors (Table 1) and most of the previously synthesized compounds (**21**–**51** in Table 2) do not

have an aryl-alkanoyl structure, typical of POP inhibitors, at the P3 and beyond P3 positions. Instead, they have rather hydrophilic P3 and beyond P3 positions, due to the amide and ketone carbonyl oxygens and the amide nitrogens. However, their modes of binding do not seem to differ from that of the typical POP inhibitors. For example, SUAM-1221 (compound **55**) occupies the binding mode A.

CoMSIA. The properties of the CoMSIA model are in agreement with the known SARs of POP inhibitors and the 3D structure of the POP enzyme.²⁷ Hydrogen bond acceptor properties (Figure 2b) are important near the electrophilic 2(*S*)-substituent of the P1 pyrrolidine ring. In the crystal structure, this substituent forms a hemiacetal bond with SER554 of POP. The thus formed oxanion is stabilized by two hydrogen bonds to the main chain NH group of Asn555 and to the hydroxyl group of Tyr473.²⁷ The P2 carbonyl oxygen is hydrogen bonded to ARG643 and the P3 carbonyl oxygen to Trp595. The P2 hydrogen bond has been proven to be crucial for the inhibitory activity.³² However, in the model, these hydrogen bonds seem to have only a small contribution to the activity. This misinformation arises from the lack of structural variation in these positions within the data set, and consequently, the real contribution to the activity cannot be revealed by the model. The binding mode B includes an area, near ARG128, where hydrogen bond acceptor properties are also favored. The formation of the hydrogen bond is not probable due to

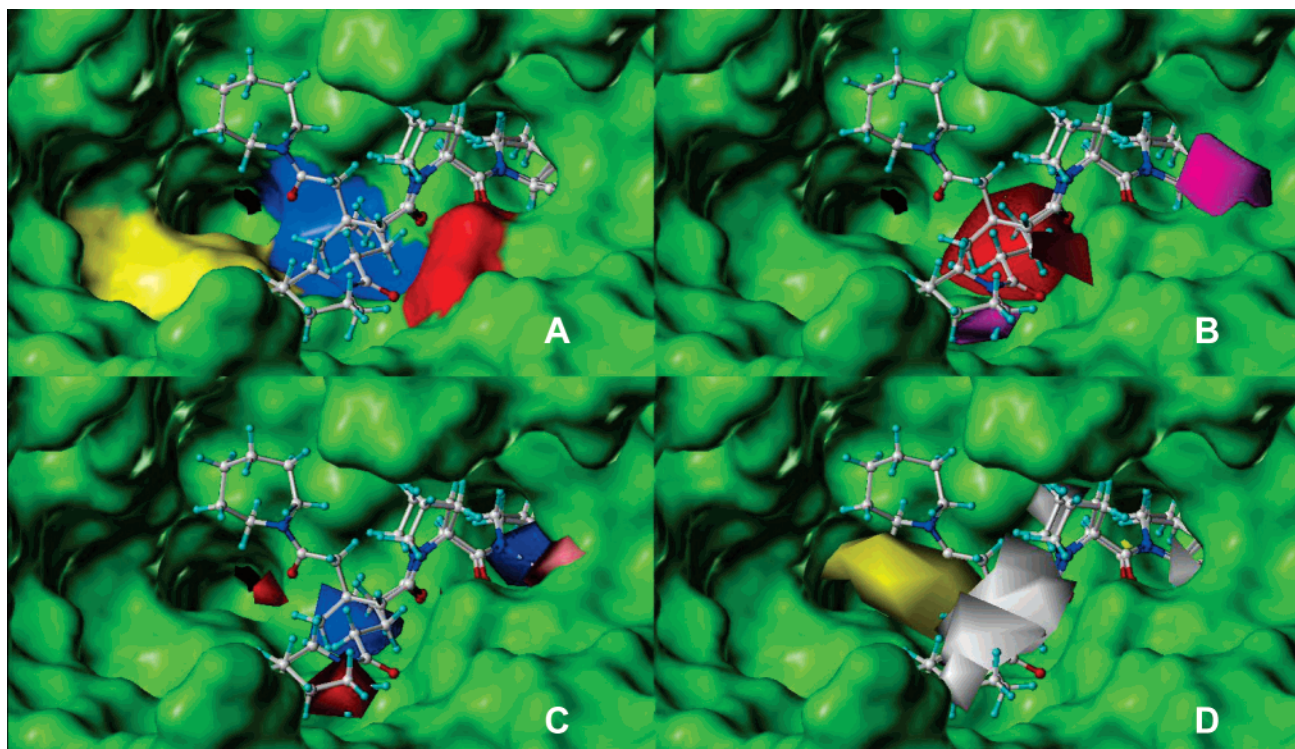


Figure 2. Most favored binding modes and the CoMSIA fields. The model compounds **14** and **15** are docked into the active site of POP. (a) Binding modes A and B are represented with compounds **15** and **14**, respectively. ILE591 and ALA594 are in blue, MET235 is in yellow, and ARG643 is in red. (b) Hydrogen bond acceptor properties. Favored areas are in magenta, and disfavored areas are in red. (c) Electrostatic properties. The partial negative charge is favored in red areas, and the partial positive charge is favored in blue areas. (d) Hydrophobic properties. Hydrophobic properties are favored in yellow areas, and hydrophilic properties are favored in white areas.

internal hydrogen bonds of POP, but the protein surface is positively charged in this area. The same area also favors partial negative charge.

Hydrogen bond acceptor properties are disfavored in the area located near the residues that do not have any hydrogen bond donors, especially the residues ILE591 (blue in Figure 2a), ALA594 (blue in Figure 2a), and MET235 (yellow in Figure 2a). Any hydrogen bond acceptor atom that points toward this area is entropically nonfavorable, since typically all polar atoms of the bound ligand have a high tendency to interact either with the receptor residues or with the surrounding water molecules.

Partial negative charge (Figure 2c) is favorable near ARG643 (red in Figure 2a), ARG128 and surprisingly near MET235 (yellow in Figure 2a). While the area near ARG643 is explained by the P2 carbonyl oxygen of an inhibitor that forms a hydrogen bond with ARG643, the area near MET235 does not seem to have a clear explanation. It may be an artifact arising from the fact that many potent inhibitors have carbonyl oxygen located in this area even though the oxygen cannot form a hydrogen bond with the enzyme. The tendency to favor partial positive charge over the carbons of the P1 prolyl ring and partial negative charge over the 2(*S*)-substituent (Figure 2c) is easily understood via the polarization between the substituent and the ring. When this polarization is strong, the interaction between the inhibitor and the SER554 becomes stronger.

Hydrophobic properties (Figure 2d) are clearly divided; the hydrophobic nature of the inhibitors is disfavored at the P1–P2 area, near the residue ARG643.

The P3 position favors lipophilic aliphatic structures. Lipophilic aromatic structures with negative π -electrons are not optimal structures but are tolerated. Beyond the P3 position, the binding mode A shows a clear hydrophobic area. The binding mode B, on the other hand, favors nonhydrophobic structures near the residue ARG128.

SARs. Three different azacycles, pyrrolidine, morpholine, and azepane, were studied at the position beyond P3, resulting in compounds **3**, **4**, and **5** respectively. A succinic acid residue was located at the P3 position and L-Pro-pyrrolidine at the P2–P1 positions. The morpholine moiety caused considerably lower potency than the azepane and pyrrolidine moieties. The replacement by an azepane moiety resulted in a more potent inhibitor than the replacement by a pyrrolidine moiety. This difference was also observed in compounds having a 2(*S*)-cyanopyrrolidine moiety at the P1 position (**11** and **12**). When the flexible succinic acid residue was changed to the rigid isophthalic acid residue (**19** and **20**), the azepane and pyrrolidine moieties gave equipotent compounds.

The polar oxygen of the morpholine ring is located in an area that favors lipophilic structures. This explains the significant decrease in inhibitory activity caused by morpholine. However, the increased lipophilicity of azepane does not explain the difference between the IC_{50} values of compounds **3** and **5**. In compound **3**, the carbonyl group next to the pyrrolidine moiety is located in an area that disfavors hydrogen bond acceptors. The carbonyl oxygen points toward the enzyme surface, which lacks hydrogen bond donors to form a bond with,

and this results in an unfavorable entropic effect. In compound **5**, the larger ring size of azepane distorts the carbonyl oxygen in a different direction, toward an open cavity. The cavity is large enough to include a water molecule that may form a hydrogen bond with the oxygen. In compounds **19** and **20**, the rigid isophthalic acid residue fixes the conformation and the inhibitors bind in a similar way to the enzyme. The phenyl group is located in an area that disfavors both lipophilic structures and negative charge, and this may explain the lower activity of compounds **19** and **20** as compared to compound **12**.

Three aliphatic chains, succinic acid, glutaric acid, and 3,3-dimethylglutaric acid, were studied at the P3 position, resulting in compounds **12**, **14**, and **15**, respectively. Azepane was used at the position beyond P3 and L-Pro-2(*S*)-cyanopyrrolidine at the P2–P1 positions. The elongation of the chain from succinic acid to glutaric acid decreased the potency. 3,3-Dimethyl glutaric acid, on the other hand, increased the potency slightly.

Compound **14** (orange in Figure 2a) seems to have a different binding mode from compounds **12** and **15** (violet in Figure 2a); the molecule turns toward the open cavity. However, the slight decrease in potency cannot be explained with the CoMSIA model. On the other hand, the increased lipophilicity of compound **15** in comparison to compound **14** may explain the increased potency in this case.

Three different substitution patterns of the phenylene moiety were studied at the P3 position, resulting in compounds **17**, **18**, and **19**. Pyrrolidine was used at the position beyond P3 and a L-Pro-2(*S*)-cyanopyrrolidine group at the P2–P1 positions. The ortho-substituted inhibitor **17** had strikingly 3 orders of magnitude lower activity than the para- and meta-substituted analogues **18** and **19**, respectively. The para-substitution resulted in the best inhibitory activity.

A rigid phenylene ring fixes the conformation, and the inhibitor cannot adjust itself to a more favorable conformation. In compound **17**, the phenylene ring is located in an area that favors hydrophilic structures. In addition, both carbonyl oxygens of the ortho-phthalic residue are located in the area that disfavors hydrogen bond acceptors.

Pyrrolidine and 2(*S*)-cyanopyrrolidine moieties were studied at the P1 position of the novel inhibitors. Inhibitors containing a 2(*S*)-cyanopyrrolidine group at the P1 position are very potent POP inhibitors.³⁵ Also in this study, the 2(*S*)-cyanopyrrolidine group increased the potency significantly as compared to a pyrrolidine group (**3** vs **11**, **5** vs **12**, **13** vs **14**, and **16** vs **17**). The interaction of the cyano group with the cystein protease papain has been studied. Cystein proteases have a similar catalytic mechanism to serine proteases. The cyano group forms a covalent, reversible thioimidate adduct with the thiol group of the active site cysteine.^{36,37} A similar interaction between the hydroxyl group of the catalytic SER554 and a cyano group is possible. Recently, the binding kinetics of compound **37** to POP was studied.³⁸ It was found to be slow binding, and the inhibition was suggested to be a direct binding process.

The role of the molecular size was studied, and the novel inhibitors were compared to the previously syn-

thesized compounds. The removal of the pyrrolidine-1-carbonyl group from compounds **21** (flexible P3 moiety) and **37** (rigid P3 moiety) resulted in compounds **3** and **19**, respectively. In both cases, the potency decreased slightly. The replacement of the L-Pro-pyrrolidine group beyond the P3 position of compounds **21**, **22**, and **37** with azepane resulted in compounds **5**, **13**, and **20**, respectively. Compounds **5** and **13** have flexible P3 moieties, and in both cases, the replacement increased the inhibitory activity. On the other hand, in the case of compound **20** with a rigid P3 moiety, the inhibitory activity decreased. Compound **20** is also less potent than the other large compounds of the same series as compound **37** (**38–42**). Interestingly, also, the small compound **54**, having only a benzoyl group at the P3 position, was slightly more active than compound **20**. The differences in the inhibitory activities between the novel compounds and the previously synthesized larger compounds were rather small and could not be explained with the CoMSIA model.

Conclusions

The P1 and P2 positions of the docked ligands were bound to POP in the same way as *Z*-L-prolyl-L-prolinal in the crystal structure. A consistent P3 position was also found. This position is surrounded by lipophilic residues, and lipophilic aliphatic structures are favored. Lipophilic aromatic structures with negative π -electrons can also be used, but then, the substitution pattern becomes crucial. Beyond the P3 position, the docked ligands divided into two different binding modes A and B, which were occupied by 60 and 40% of the inhibitors, respectively. According to the previously postulated idea of the lipophilic cavity, the binding mode A favors lipophilic structures. The binding mode B instead favors nonhydrophobic structures, and partial negative charge is favored near ARG128, where the protein surface has a partial positive charge. The P3 and beyond P3 area is sufficiently large, and the interactions between POP and the ligands are weak. This area can accommodate several different groups without affecting the inhibitory activity and could be a valuable modification site for the optimization of ADME properties. The docking studies with the 3D QSAR models are helpful in the design of new compounds.

Experimental Section

General Methods. ¹H and ¹³C NMR spectra were recorded on a Bruker AM 400 WB or a Bruker Avance 500 spectrometer. Chemical shifts (δ) are given in ppm downfield from the internal standard tetramethylsilane (δ 0.00). Electrospray ionization mass spectra (ESI-MS) were obtained on a LCQ ion trap mass spectrometer equipped with an ESI source (Finnigan MAT, San Jose, CA). Elemental analyses (C, H, N) were carried out with a Thermo Quest CE Instruments EA 1110 CHNS-O elemental analyzer. Flash chromatography was performed on J. T. Bakers silica gel for chromatography (pore size 60 Å, particle size 50 μ m). The silica plate for the chromatotron was made of Merck silica gel 60 PF₂₅₄-containing gypsum (particle size 5–40 μ m).

The N-amide bond of a proline residue or a 2-substituted pyrrolidine moiety has energetically similar cis and trans isomers (rotamers). These rotamers have slightly different shifts. This is best seen in the ¹³C NMR spectra of compound **16** where two rotamers raise two signals for each carbon of the compound. Minor rotamers that are less than 20% of the size of the major rotamers are not reported.

General Synthesis Procedure A. A solution of 1.0 equiv of pivaloyl chloride in dichloromethane (DCM) was added to a solution of 1.0 equiv of carboxylic acid and 1.1 equiv of triethylamine in DCM at 0 °C. The reaction mixture was stirred at 0 °C for 1 h. A solution of 1.1 equiv of triethylamine and 1.0–1.1 equiv of amine in DCM was slowly added at 0 °C (if the amine was in the form of a trifluoroacetic acid salt or HCl salt, then 3.3 equiv of triethylamine was used and the triethylamine was added separately before the amine was added). The reaction mixture was stirred 2 h or overnight at room temperature. The DCM solution was washed with 30% citric acid (aq), saturated NaCl (aq), and saturated NaHCO₃ (aq), dried over anhydrous Na₂SO₄, and evaporated, yielding the crude product.

General Synthesis Procedure B. A 1.0–1.5 equiv amount of LiOH·H₂O was added to a solution of 1.0 equiv of carboxylic acid methyl ester in 20–30% water in methanol. The reaction was stirred 2 h or overnight at room temperature. The solvent (methanol) was evaporated, and the residue was dissolved in water. The aqueous phase was washed with DCM. The aqueous phase was made acidic with 2–3 M HCl (aq), and the product was extracted with DCM. The organic phase was dried over anhydrous Na₂SO₄ and evaporated, yielding the product.

General Synthesis Procedure C. A 2–4 mL amount of ethyl acetate saturated with dry HCl was added to 1.0 mmol of BOC-protected amine at room temperature. The reaction mixture was stirred at room temperature for 30 min. Another way to proceed was to dissolve 1.0 mmol of BOC-protected amine in 5–10 mL of DCM and add 2–4 mL of trifluoroacetic acid at 0 °C. The reaction was stirred at 0 °C for 2–2.5 h. In both cases, the solvent was removed and the product was finally evaporated in vacuo, yielding the corresponding amine HCl salt or TFA salt.

BOC-L-prolyl-pyrrolidine (1). BOC-L-proline (7.97 g, 37.0 mmol) and pyrrolidine (3.09 mL, 37.0 mmol) were coupled according to procedure A. The product was purified by column chromatography (2.5–5% MeOH in DCM). Yield: 8.31 g, 84%.

Succinic Acid Monomethyl Ester L-Prolyl-pyrrolidine Amide (2). BOC-L-prolyl-pyrrolidine (1.98 g, 7.4 mmol) was deprotected using 30 mL of HCl-saturated ethyl acetate according to procedure C. Succinic acid monomethyl ester (0.98 g, 7.4 mmol) and the L-prolyl-pyrrolidine HCl salt were coupled according to procedure A. The product was purified by column chromatography (5–10% MeOH in EtOAc). Yield: 1.81 g, 86%.

Succinic Acid Pyrrolidine L-Prolyl-pyrrolidine Amide (3). The methyl ester group of **2** (750 mg, 2.7 mmol) was hydrolyzed using LiOH·H₂O (170 mg, 4.1 mmol) according to procedure B. Yield: 360 mg, 1.3 mmol, 45%. The obtained product was coupled with pyrrolidine (0.11 mL, 1.3 mmol) according to procedure A. The product was purified by column chromatography (25% MeOH in EtOAc). Yield: 170 mg, 41%. ¹H NMR (500.1 MHz, CDCl₃): δ 1.79–2.18 (10 H, m), 2.23–2.45 (2 H, m), 2.47–2.68 (2 H, m), 2.78–2.92 (2 H, m), 3.39–3.62 (7 H, m), 3.64–3.84 (3 H, m), 4.68 (dd, 0.9 H, *J* = 3.8 Hz, 8.4), 4.77 (dd, 0.1 H, *J* = 3.0 Hz, 8.8 Hz). ¹³C NMR (125.1 MHz, CDCl₃): δ 24.1, 24.4, 24.8, 26.0, 26.2, 28.9, 29.2, 29.3, 45.7, 45.9, 46.2, 46.4, 47.3, 57.8, 170.5, 170.7, 170.8. MS (ESI, +) *m/z* 322 [M + H]⁺. Anal. (C₁₇H₂₇N₃O₃) C, H, N.

Succinic Acid Morpholine L-Prolyl-pyrrolidine Amide (4). The methyl ester group of **2** (560 mg, 2.0 mmol) was hydrolyzed using LiOH·H₂O (84 mg, 2.0 mmol) in 10 mL of 20% water in MeOH at room temperature. After 4 h, the solvent was evaporated and the residue was dissolved in DCM. The organic phase was dried and evaporated. The obtained product was coupled with morpholine (0.18 mL, 2.0 mmol) according to procedure A. The product was purified by column chromatography (20–25% MeOH in EtOAc). Yield: 330 mg, 49%. ¹H NMR (400.1 MHz, CDCl₃): δ 1.80–2.05 (6 H, m), 2.08–2.35 (2 H, m), 2.39–2.64 (2 H, m), 2.78–2.95 (2 H, m), 3.35–3.81 (14 H, m), 4.64 (0.9 H, dd, *J* = 3.8 Hz, 8.3 Hz), 4.69 (0.1 H, dd, *J* = 3.8 Hz, 8.5 Hz). ¹³C NMR (125.1 MHz, CDCl₃): δ 24.1, 24.8, 26.2, 27.7, 28.9, 29.3, 42.2, 45.8, 46.1, 46.4, 47.4, 58.0, 66.6, 66.9, 170.9, 171.0, 171.1. MS (ESI, +) *m/z* 338 [M + H]⁺. Anal. (C₁₇H₂₇N₃O₄·0.3H₂O) C, H, N.

Succinic Acid Azepane L-Prolyl-pyrrolidine Amide (5). The methyl ester group of **2** (560 mg, 2.0 mmol) was hydrolyzed using LiOH·H₂O (84 mg, 2.0 mmol) in 10 mL of 20% water in MeOH at room temperature. After 3 h, the solvent was evaporated and the residue was dissolved in DCM. The organic phase was dried and evaporated. The obtained product was coupled with azepane (0.23 mL, 2.0 mmol) according to procedure A. The product was purified by column chromatography (20% MeOH in EtOAc). Yield: 350 mg, 50%. ¹H NMR (500.1 MHz, CDCl₃): δ 1.51–1.61 (4 H, m), 1.64–1.77 (4 H, m), 1.81–2.45 (8 H, m), 2.51–2.64 (2 H, m), 2.80–2.88 (2 H, m), 3.36–3.90 (10 H, m), 4.65 (0.9 H, dd, *J* = 3.8 Hz, 8.4 Hz), 4.71 (0.1 H, dd, *J* = 3.1 Hz, 8.6 Hz). ¹³C NMR (125.1 MHz, CDCl₃): δ 24.1, 24.8, 26.2, 26.9, 27.1, 27.6, 28.0, 28.9, 29.0, 29.6, 45.9, 46.0, 46.3, 47.2, 47.7, 57.8, 170.7, 170.9, 171.6. MS (ESI, +) *m/z* 350 [M + H]⁺. Anal. (C₁₉H₃₁N₃O₃·0.2H₂O) C, H, N.

Phthalic Acid Mono-(L-proline methyl ester) Amide (6). Phthalic acid anhydride (7.4 g, 45 mmol) was added to a solution of L-proline methyl ester HCl salt (7.4 g, 45 mmol) and triethylamine (13.8 mL, 99 mmol) in DCM at 0 °C. The reaction mixture was stirred for 4 h at room temperature. The organic phase was extracted with saturated NaHCO₃ (aq). The aqueous phase was acidified with 3 M HCl (aq) and extracted with chloroform. The chloroform phase was dried and evaporated. Yield: 6.53 g, 51%.

Succinic Acid Monopyrrolidine Amide (7a). Succinic acid monomethyl ester (1.98 g, 15 mmol) and pyrrolidine (1.3 mL, 15 mmol) were coupled according to procedure A. The product was purified by column chromatography (EtOAc). Yield: 1.75 g, 63%. The methyl ester group of the product was hydrolyzed using LiOH·H₂O (0.44 g, 10.4 mmol) according to procedure B. Yield: 1.37 g, 85%.

Isophthalic Acid Monopyrrolidine Amide (7b). Iso-phthalic acid monomethyl ester (2.25 g, 12.5 mmol) and pyrrolidine (1.04 mL, 12.5 mmol) were coupled according to procedure A. The product was purified by column chromatography (30% petroleum ether in EtOAc). Yield: 1.75 g, 60%. The methyl ester group of the product was hydrolyzed using LiOH·H₂O (470 mg, 11.3 mmol) according to procedure B. Yield: 1.49 g, 91%.

Terephthalic Acid Monopyrrolidine Amide (7c). Terephthalic acid monomethyl ester (1.08 g, 6.0 mmol) and pyrrolidine (0.50 mL, 6.0 mmol) were coupled according to procedure A. The product was purified by column chromatography (EtOAc). Yield: 0.50 g, 36%. The methyl ester group of the product was hydrolyzed using LiOH·H₂O (135 mg, 3.2 mmol) according to procedure B. Yield: 0.41 g, 87%.

Succinic Acid Monoazepane Amide (8a). Succinic acid monomethyl ester (1.98 g, 15 mmol) and azepane (1.7 mL, 15 mmol) were coupled according to procedure A. The product was purified by column chromatography (30% petroleum ether in EtOAc). Yield: 2.48 g, 78%. The methyl ester group of the product was hydrolyzed using LiOH·H₂O (540 mg, 12.9 mmol) according to procedure B. Yield: 2.34 g, 100%.

Isophthalic Acid Monoazepane Amide (8b). Isophthalic acid monomethyl ester (2.25 g, 12.5 mmol) and azepane (1.41 mL, 12.5 mmol) were coupled according to procedure A. The product was purified by column chromatography (40% petroleum ether in EtOAc). Yield: 2.02 g, 62%. The methyl ester group of the product was hydrolyzed using LiOH·H₂O (490 mg, 11.7 mmol) according to procedure B. Yield: 1.89 g, 99%.

Glutaric Acid Monoazepane Amide (8c). To a solution of azepane (4.5 mL, 40 mmol) in 40 mL of THF was added glutaric anhydride (2.3 g, 20 mmol) in 15 mL of THF dropwise, and the solution was stirred for 2 days. The reaction mixture was evaporated, dissolved in 0.025 M NaOH (aq), and washed with DCM. The aqueous phase was acidified with 3 M HCl, and the product was extracted with DCM. The combined organic phases were dried and evaporated. Yield: 1.61 g, 38%.

3,3-Dimethylglutaric Acid Monoazepane Amide (8d). To a solution of azepane (1.74 mL, 15.4 mmol) in 10 mL of THF was added 3,3-dimethylglutaric anhydride (1.0 g, 7 mmol) in 10 mL of THF dropwise at 0 °C. The reaction mixture was

stirred overnight at room temperature, evaporated, and dissolved in 0.025 M NaOH (aq). The water phase was washed with DCM, acidified with 3 M HCl (aq), and extracted with DCM. The organic phase was dried and evaporated, yielding solid product: 1.53 g, 90%.

Succinic Acid Pyrrolidine L-Proline Amide (9a). Compound **7a** (1.37 g, 8.0 mmol) was coupled with proline methyl ester HCl salt (1.3 g, 8.0 mmol) according to procedure A. The product was purified by column chromatography (5% MeOH in DCM). Yield: 1.45 g, 64%. The methyl ester group of the product was hydrolyzed using LiOH·H₂O (0.32 g, 7.65 mmol) according to procedure B. Yield: 1.32 g, 96%.

Isophthalic Acid Pyrrolidine L-Proline Amide (9b). Compound **7b** (1.49 g, 6.8 mmol) and proline methyl ester HCl salt (1.13 g, 6.8 mmol) were coupled according to procedure A. The product was purified by column chromatography (10% MeOH in EtOAc). Yield: 1.83 g, 81%. The methyl ester group of the product was hydrolyzed using LiOH·H₂O (350 mg, 8.3 mmol) according to procedure B. Yield: 1.58 g, 91%.

Terephthalic Acid Pyrrolidine L-Proline Amide (9c). Compound **7c** (0.41 g, 1.9 mmol) and l-proline methyl ester HCl salt (0.31 g, 1.9 mmol) were coupled according to procedure A. The product was purified by column chromatography (10% MeOH in EtOAc). Yield: 0.54 g, 87%. The methyl ester group of the product was hydrolyzed using LiOH·H₂O (103 mg, 2.5 mmol) according to procedure B. Yield: 0.50 g, 97%.

Phthalic Acid Pyrrolidine L-Proline Amide (9d). Compound **6** (4.25 g, 17.0 mmol) and pyrrolidine (1.6 mL, 18.7 mmol) were coupled according to procedure A. The product was purified by column chromatography (5–20% MeOH in EtOAc). Yield: 4.77 g, 85%. The methyl ester group of the product was hydrolyzed using LiOH·H₂O (906 mg, 21.6 mmol) according to procedure B. Yield: 3.42 g, 75%.

Succinic Acid Azepane L-Proline Amide (10a). Compound **8a** (2.34 g, 11.7 mmol) was coupled with proline methyl ester HCl salt (1.9 g, 11.7 mmol) according to procedure A. The product was purified by column chromatography (5% MeOH in DCM). Yield: 2.22 g, 61%. The methyl ester group of the product was hydrolyzed using LiOH·H₂O (0.45 g, 10.7 mmol) according to procedure B. Yield: 2.01 g, 95%.

Isophthalic Acid Azepane L-Proline Amide (10b). Compound **8b** (1.89 g, 7.6 mmol) and proline methyl ester HCl salt (1.27 g, 7.6 mmol) were coupled according to procedure A. The product was purified by column chromatography (10% MeOH in EtOAc). Yield: 2.08 g, 76%. The methyl ester group of the product was hydrolyzed using LiOH·H₂O (370 mg, 8.7 mmol) according to procedure B. Yield: 1.67 g, 83%.

Glutaric Acid Azepane L-Proline Amide (10c). Compound **8c** (1.61 g, 7.5 mmol) and l-proline methyl ester HCl salt (1.24 g, 7.5 mmol) were coupled according to procedure A. The product was purified by column chromatography (5–10% MeOH in EtOAc) to give the product as colorless oil. Yield: 1.8 g, 74%. The methyl ester group of the product (1.8 g, 5.6 mmol) was hydrolyzed using LiOH·H₂O (0.35 g, 8.3 mmol) according to procedure B. Yield: 1.55 g, 90%.

3,3-Dimethylglutaric Acid Azepane L-Proline Amide (10d). Compound **8d** (0.50 g, 2.1 mmol) and l-proline methyl ester HCl salt (0.34 g, 2.1 mmol) were coupled according to procedure A. The product was purified by column chromatography (25–50% EtOAc in petroleum ether). Yield: 0.55 g, 75%. The methyl ester group of the product (0.55 g, 1.6 mmol) was hydrolyzed using LiOH·H₂O (0.10 g, 2.4 mmol) according to procedure B. Yield: 0.52 g, 96%.

Succinic Acid Pyrrolidine L-Prolyl-2(S)-cyanopyrrolidine Amide (11). BOC-2(S)-cyanopyrrolidine (0.96 g, 4.9 mmol) was deprotected using 20 mL of trifluoroacetic acid in 50 mL of DCM according to procedure C. 2(S)-cyanopyrrolidine TFA salt was coupled with **9a** (1.32 g, 4.9 mmol) according to procedure A. The product was purified by column chromatography (10% MeOH in EtOAc). Yield: 170 mg, 10%. ¹H NMR (500.1 MHz, CDCl₃): δ 1.81–1.86 (2 H, m), 1.91–2.05 (4 H, m), 2.12–2.32 (6 H, m), 2.42–2.54 (2 H, m), 2.73–2.88 (2 H, m), 3.36–3.48 (4 H, m), 3.60–3.63 (1 H, m), 3.66–3.75 (2 H, m), 3.82–3.86 (1 H, m), 4.59 (1 H, dd, *J* = 4.0 Hz, 8.4 Hz),

4.78–4.82 (1 H, m). ¹³C NMR (125.1 MHz, CDCl₃): δ 24.4, 24.8, 25.4, 26.0, 27.7, 29.1, 29.3, 29.7, 45.7, 46.3, 46.4, 46.5, 47.3, 57.5, 118.6, 170.3, 171.2, 171.4. MS (ESI, +) *m/z* 369 [M + Na]⁺. Anal. (C₁₈H₂₆N₄O₃·0.1H₂O) C, H, N: calcd, 16.09; found, 15.57.

Succinic Acid Azepane L-Prolyl-2(S)-cyanopyrrolidine Amide (12). BOC-2(S)-cyanopyrrolidine (1.3 g, 6.8 mmol) was deprotected using 27 mL of trifluoroacetic acid in 70 mL of DCM according to procedure C. Compound **10a** (2.01 g, 6.8 mmol) and the 2(S)-cyanopyrrolidine trifluoroacetic acid salt were coupled according to procedure A. The product was purified by column chromatography (8–10% MeOH in EtOAc). Yield: 320 mg, 13%. ¹H NMR (400.1 MHz, CDCl₃): δ 1.47–1.59 (4 H, m), 1.62–1.76 (4 H, m), 1.92–2.06 (2 H, m), 2.10–2.33 (6 H, m), 2.45–2.58 (2 H, m), 2.76–2.89 (2 H, m), 3.35–3.87 (8 H, m), 4.58 (1 H, dd, *J* = 3.7 Hz, 8.1 Hz), 4.80–4.83 (1 H, m). ¹³C NMR (125.1 MHz, CDCl₃): δ 24.8, 25.4, 26.9, 27.1, 27.6, 27.9, 28.7, 29.0, 29.5, 29.7, 46.0, 46.3, 46.5, 47.3, 47.7, 57.5, 118.6, 171.2, 171.3, 171.4. MS (ESI, +) *m/z* 375 [M + H]⁺. Anal. (C₂₀H₃₀N₄O₃·0.2H₂O) C, H, N.

Glutaric Acid Azepane L-Prolyl-pyrrolidine Amide (13). Compound **10c** (0.51 g, 1.6 mmol) was coupled with pyrrolidine (0.14 mL, 1.7 mmol) according to procedure A. The product was purified by column chromatography (15% MeOH in EtOAc) to give the product as colorless oil. Yield: 0.34 g, 57%. ¹H NMR (500.1 MHz, CDCl₃): δ 1.51–1.58 (4 H, m), 1.65–1.74 (4 H, m), 1.78–2.29 (10 H, m), 2.31–2.48 (4 H, m), 3.35–3.72 (9 H, m), 3.80–3.85 (1 H, m), 4.57 (0.1 H, dd, *J* = 2.8 Hz, 8.8 Hz), 4.64 (0.9 H, dd, *J* = 3.8 Hz, 8.4 Hz). ¹³C NMR (125.1 MHz, CDCl₃): δ 20.4, 24.1, 24.9, 26.2, 26.9, 27.2, 27.7, 28.9, 29.2, 32.3, 33.8, 45.9, 45.9, 46.3, 47.4, 47.9, 57.7, 170.7, 171.4, 172.3. MS (ESI, +) *m/z* 364 [M + H]⁺. Anal. (C₂₀H₃₃N₃O₃·0.1H₂O) C, H, N.

Glutaric Acid Azepane L-Prolyl-L-proline Amide. Compound **10c** (0.38 g, 1.2 mmol) and l-proline methyl ester HCl salt (0.20 g, 1.2 mmol) were coupled according to procedure A. The product was purified by column chromatography (10–20% MeOH in EtOAc) to give the product as oil. Yield: 0.42 g, 82%. The methyl ester group of the obtained product was hydrolyzed using LiOH·H₂O (63 mg, 1.5 mmol) according to procedure B to give the white solid product. Yield: 0.39 g, 95%.

Glutaric Acid Azepane L-Prolyl-L-prolinamide Amide. To a solution of glutaric acid azepane l-prolyl-l-proline amide (170 mg, 0.42 mmol) and Et₃N (59 μL, 0.42 mmol) in 8 mL of THF was added ethyl chloroformate (40 μL, 0.42 mmol) in 4 mL of THF dropwise at –10 °C. After 20 min, 25% NH₃ (aq) (143 μL, 2.1 mmol) was added and the reaction mixture was stirred overnight at room temperature. The reaction mixture was evaporated, dissolved in DCM, and filtered. The filtrate was washed with saturated NaHCO₃ (aq), dried, and evaporated yielding the white solid product (150 mg, 88%).

Glutaric Acid Azepane L-Prolyl-2(S)-cyanopyrrolidine Amide (14). To a solution of glutaric acid azepane l-prolyl-l-prolinamide amide (150 mg, 0.37 mmol) and Et₃N (155 μL, 1.11 mmol) in 8 mL of THF was added trifluoroacetic anhydride (80 μL, 0.56 mmol) in 4 mL of THF dropwise at 0 °C. The reaction mixture was stirred 2 h at room temperature, evaporated, and dissolved in DCM. The organic phase was washed with 30% citric acid (aq), dried, and evaporated. The product was purified by column chromatography (10% MeOH in EtOAc) yielding colorless oil (76 mg, 53%). ¹H NMR (500.1 MHz, CDCl₃): δ 1.52–1.59 (4 H, m), 1.66–1.73 (4 H, m), 1.90–2.06 (4 H, m), 2.09–2.31 (6 H, m), 2.35–2.47 (4 H, m), 3.39–3.44 (2 H, m), 3.45–3.64 (4 H, m), 3.66–3.71 (1 H, m), 3.85–3.90 (1 H, m), 4.55 (0.9 H, dd, *J* = 4.2 Hz, 8.6 Hz), 4.60–4.62 (0.1 H, m), 4.65–4.68 (0.1 H, m), 4.79–4.81 (0.9 H, m). ¹³C NMR (125.1 MHz, CDCl₃): δ 20.3, 25.0, 25.4, 26.9, 27.2, 27.7, 28.8, 29.1, 29.7, 32.1, 33.7, 45.9, 46.3, 46.5, 47.4, 47.8, 57.4, 118.6, 171.4, 171.7, 172.1. MS (ESI, +) *m/z* 389 [M + H]⁺. Anal. (C₂₁H₃₂N₄O₃·0.2H₂O) C, H, N.

3,3-Dimethylglutaric Acid Azepane L-Prolyl-L-proline Amide. Compound **10d** (0.52 g, 1.5 mmol) and l-proline methyl ester HCl salt (0.26 g, 1.5 mmol) were coupled according to procedure A. The product was purified by column

chromatography (10% MeOH in EtOAc). Yield: 0.54 g, 78%. The methyl ester group of the obtained product was hydrolyzed using LiOH·H₂O (76 mg, 1.8 mmol) according to procedure B. Yield: 0.54 g, 100%.

3,3-Dimethylglutaric Acid Azepane L-Prolyl-L-prolinamide Amide. To a solution of 3,3-dimethylglutaric acid azepane L-prolyl-L-proline amide (0.54 g, 1.2 mmol) and Et₃N (0.17 mL, 1.2 mmol) in THF was added ethyl chloroformate (0.12 mL, 1.3 mmol) in THF dropwise at -10 °C. After 20 min, 25% NH₃ (aq) (84 μL, 1.2 mmol) was added and the reaction mixture was allowed to warm to room temperature and stirred overnight. The reaction mixture was evaporated, dissolved in DCM, and washed with saturated NaHCO₃ (aq). The organic phase was dried and evaporated. Yield: 450 mg, 84%.

3,3-Dimethylglutaric Acid Azepane L-Prolyl-2(S)-cyano-pyrrolidine Amide (15). To a solution of 3,3-dimethylglutaric acid azepane L-prolyl-L-prolinamide amide (0.45 g, 1.0 mmol) and Et₃N (0.43 mL, 3.1 mmol) in THF was added trifluoroacetic anhydride (0.22 mL, 1.6 mmol) in THF dropwise at 0 °C. The reaction mixture was stirred for 6 h at room temperature, and the reaction was then quenched with 5 mL of water. The reaction mixture was evaporated, dissolved in DCM, and washed with 30% citric acid (aq), saturated NaCl (aq), and saturated NaHCO₃ (aq). The organic phase was dried and evaporated. The product was purified by column chromatography (30–50% ACN in EtOAc), yielding white solid: 250 mg, 58%. ¹H NMR (500.1 MHz, CDCl₃): δ 1.17 (3 H, s), 1.18 (3 H, s), 1.51–1.58 (4 H, m), 1.67–1.73 (4 H, m), 1.90–1.98 (2 H, m), 2.09–2.28 (6 H, m), 2.35–2.64 (4 H, m), 3.40–3.75 (7 H, m), 3.82–3.87 (1 H, m), 4.56 (0.9 H, dd, *J* = 4.3 Hz, 8.4 Hz), 4.73–4.86 (1.1 H, m). ¹³C NMR (125.1 MHz, CDCl₃): δ 25.0, 25.4, 26.8, 27.0, 27.7, 28.5, 28.6, 28.7, 29.1, 29.7, 34.0, 42.1, 43.8, 45.9, 46.2, 46.5, 48.1, 48.4, 57.4, 118.7, 171.1, 171.4, 171.5. MS (ESI, +) *m/z* 417 [M + H]⁺. Anal. (C₂₃H₃₆N₄O₃·0.1H₂O) C, H, N.

Phthalic Acid Pyrrolidine L-Prolyl-pyrrolidine Amide (16). Compound **9d** (0.90 g, 2.8 mmol) was coupled with pyrrolidine (0.26 mL, 3.1 mmol) according to procedure A. The product was purified by column chromatography (10% MeOH in EtOAc). Yield: 860 mg, 83%. ¹H NMR (500.1 MHz, CDCl₃): δ 1.49–1.58 (1 H, m), 1.65–1.74 (1 H, m), 1.81–2.06 (8 H, m), 2.14–2.29 (1.5 H, m), 2.48–2.52 (0.5 H, m), 3.00–3.05 (0.5 H, m), 3.14–3.89 (9.5 H, m), 4.69 (0.5 H, dd, *J* = 3.3 Hz, 8.2 Hz), 4.79 (0.5 H, dd, *J* = 6.2 Hz, 8.3 Hz), 7.29–7.42 (3.5 H, m), 7.51–7.55 (0.5 H, m). ¹³C NMR (125.1 MHz, CDCl₃): δ 23.3, 24.0, 24.2, 24.5, 24.6, 25.2, 25.9, 25.9, 26.0, 26.2, 29.2, 30.5, 45.6, 45.6, 45.7, 45.7, 46.0, 46.3, 46.8, 48.8, 48.9, 49.8, 57.6, 59.4, 125.7, 126.4, 127.4, 127.5, 128.5, 128.7, 128.9, 128.9, 135.2, 135.6, 135.7, 135.8, 168.6, 168.7, 168.8, 169.0, 170.3, 171.1. MS (ESI, +) *m/z* 370 [M + H]⁺. Anal. (C₂₁H₂₇N₃O₃·0.2H₂O) C, H, N.

Phthalic Acid Pyrrolidine L-Prolyl-2(S)-cyanopyrrolidine Amide (17). BOC-2(S)-cyanopyrrolidine (980 mg, 5.0 mmol) was deprotected using 10 mL of trifluoroacetic acid in 50 mL of DCM according to procedure C. Compound **9d** (1.58 g, 5.0 mmol) and the 2(S)-cyanopyrrolidine trifluoroacetic acid salt were coupled according to procedure A. The product was purified with a silica plate chromatotron (2% MeOH in DCM). Yield: 250 mg, 13%. ¹H NMR (400.1 MHz, CDCl₃): δ 1.65–2.12 (8 H, m), 2.15–2.33 (4 H, m), 3.11–3.37 (2 H, m), 3.42–3.73 (5 H, m), 3.79–3.94 (1 H, m), 4.43–4.45 (0.3 H, m), 4.72 (0.7 H, dd, *J* = 6.3 Hz, 8.3 Hz), 4.77 (0.3 H, dd, *J* = 3.4 Hz, 8.2 Hz), 4.81–4.84 (0.7 H, m), 7.26–7.33 (1 H, m), 7.34–7.44 (2 H, m), 7.46–7.51 (1 H, m). ¹³C NMR (100.6 MHz, CDCl₃): δ 24.6, 25.3, 25.4, 26.0, 29.2, 29.7, 45.7, 46.3, 46.6, 49.0, 49.7, 57.4, 118.6, 126.5, 127.2, 129.1, 129.1, 135.4, 135.7, 168.6, 168.9, 171.0. MS (ESI, +) *m/z* 395 [M + H]⁺. Anal. (C₂₂H₂₆N₄O₃·0.2H₂O) C, H, N.

Terephthalic Acid Pyrrolidine L-Prolyl-L-proline Amide. Compound **9c** (0.50 g, 1.6 mmol) and L-proline methyl ester HCl salt (0.27 g, 1.6 mmol) were coupled according to procedure A. The product was purified by column chromatography (5–10% MeOH in EtOAc). Yield: 0.45 g, 66%. The methyl ester

group of the product was hydrolyzed using LiOH·H₂O (69 mg, 1.6 mmol) according to procedure B. Yield: 0.43 g, 95%.

Terephthalic Acid Pyrrolidine L-Prolyl-L-prolinamide Amide. The compound was prepared from terephthalic acid pyrrolidine L-prolyl-L-proline amide (0.43 g, 1.0 mmol) and 25% NH₃ (aq) (71 μL, 1.0 mmol) according to the method for preparation of 3,3-dimethylglutaric acid azepane l-prolyl-L-prolinamide amide. The product was purified by column chromatography (10–30% MeOH in EtOAc). Yield: 260 mg, 61%.

Terephthalic Acid Pyrrolidine L-Prolyl-2(S)-cyano-pyrrolidine Amide (18). Compound **18** was prepared from terephthalic acid pyrrolidine L-prolyl-L-prolinamide amide (0.26 g, 0.63 mmol) according to the method for the preparation of **15**. The reaction time was 2 h. The product was purified by column chromatography (30–50% ACN in EtOAc), yielding yellowish solid: 145 mg, 59%. ¹H NMR (500.1 MHz, CDCl₃): δ 1.86–2.33 (12 H, m), 3.22–3.26 (0.1 H, m), 3.33 (0.2 H, t, *J* = 6.6 Hz), 3.38 (1.8 H, t, *J* = 6.6 Hz), 3.50–3.55 (1 H, m), 3.60–3.91 (4.0 H, m), 3.70–4.02 (0.9 H, m), 4.27–4.29 (0.1 H, m), 4.39–4.41 (0.1 H, m), 4.75 (0.9 H, dd, *J* = 6.1 Hz, 8.0 Hz), 4.85–4.87 (0.9 H, m), 7.37–7.39 (0.2 H, m), 7.43–7.45 (0.2 H, m), 7.54–7.55 (1.8 H, m), 7.58–7.60 (1.8 H, m). ¹³C NMR (125.1 MHz, CDCl₃): δ 24.4, 25.4, 25.6, 26.4, 29.0, 29.8, 46.2, 46.5, 46.6, 49.5, 50.2, 58.0, 118.6, 127.1, 127.3, 137.3, 139.0, 168.8, 168.9, 171.1. MS (ESI, +) *m/z* 395 [M + H]⁺. Anal. (C₂₂H₂₆N₄O₃·0.5H₂O) C, H, N.

Isophthalic Acid Pyrrolidine L-Prolyl-2(S)-cyano-pyrrolidine Amide (19). BOC-2(S)-cyanopyrrolidine (980 mg, 5.0 mmol) was deprotected using 20 mL of trifluoroacetic acid in 50 mL of DCM according to procedure C. Compound **9b** (1.58 g, 5.0 mmol) and the 2(S)-cyanopyrrolidine trifluoroacetic acid salt were coupled according to procedure A. The product was purified by column chromatography (1.5–3% MeOH in DCM). Yield: 730 mg, 37%. ¹H NMR (500.1 MHz, CDCl₃): δ 1.82–2.13 (7 H, m), 2.15–2.32 (5 H, m), 3.21–3.43 (2 H, m), 3.53–3.90 (5 H, m), 3.98–4.02 (1 H, m), 4.25–4.27 (0.2 H, m), 4.55–4.57 (0.2 H, m), 4.75 (0.8 H, dd, *J* = 6.3 Hz, 8.1 Hz), 4.85–4.87 (0.8 H, m), 7.43–7.47 (1 H, m), 7.58–7.62 (2 H, m), 7.68–7.69 (1 H, m). ¹³C NMR (100.6 MHz, CDCl₃): δ 24.5, 25.4, 25.7, 26.4, 29.0, 29.8, 46.2, 46.5, 46.6, 49.6, 50.3, 58.0, 118.6, 125.8, 128.5, 128.6, 129.0, 136.1, 137.5, 168.8, 168.8, 171.1. MS (ESI, +) *m/z* 395 [M + H]⁺. Anal. (C₂₂H₂₆N₄O₃·0.2H₂O) C, H, N.

Isophthalic Acid Azepane L-Prolyl-2(S)-cyanopyrrolidine Amide (20). BOC-2(S)-cyanopyrrolidine (940 mg, 4.8 mmol) was deprotected using 19 mL of trifluoroacetic acid in 50 mL of DCM according to procedure C. Compound **10b** (1.67 g, 4.8 mmol) and the 2(S)-cyanopyrrolidine trifluoroacetic acid salt were coupled according to procedure A. The product was purified by column chromatography (1.5–2.5% MeOH in DCM). Yield: 920 mg, 45%. ¹H NMR (500.1 MHz, CDCl₃): δ 1.53–1.66 (6 H, m), 1.78–2.32 (10 H, m), 3.21–3.35 (2 H, m), 3.53–3.90 (5 H, m), 3.97–4.02 (1 H, m), 4.24–4.26 (0.2 H, m), 4.53 (0.2 H, dd, *J* = 3.3 Hz, 6.8 Hz), 4.74 (0.8 H, dd, *J* = 6.4 Hz, 7.9 Hz), 4.85–4.87 (0.8 H, m), 7.42–7.45 (2 H, m), 7.56–7.60 (2 H, m). ¹³C NMR (100.6 MHz, CDCl₃): δ 25.4, 25.7, 26.5, 27.2, 27.8, 29.0, 29.4, 29.8, 46.3, 46.5, 46.6, 49.8, 50.3, 58.0, 118.6, 125.3, 127.9, 128.3, 128.6, 136.2, 137.6, 168.8, 170.6, 171.1. MS (ESI, +) *m/z* 423 [M + H]⁺. Anal. (C₂₄H₃₀N₄O₃·0.1H₂O) C, H, N.

In Vitro Assay of POP Inhibitory Activity. The whole porcine brains, excluding cerebellum and most of the brain stem, were placed in liquid nitrogen within 30 min after the animals were killed and stored at -80 °C until homogenized. The brains were homogenized in 3 volumes (w/v) of ice-cold 0.1 M sodium-potassium phosphate buffer (pH 7.0), and the homogenates were centrifuged for 20 min at 4 °C at 10000g. The supernatants were pooled and stored in small aliquots at -80 °C until used. The supernatant was thawed in ice just before it was used in the activity assay and diluted in a ratio 1:2 with homogenization buffer.

Inhibitors were dissolved in DMSO to 0.01 M, and further dilutions were made in assay buffer. The highest final DMSO concentration in all but one case (compound **16**) was 0.1% or

below (at inhibitor concentration of 10 μM), which caused negligible POP inhibition.³⁹ For compound **16**, the highest final DMSO concentration was 1% (at inhibitor concentration of 100 μM), which inhibits POP by 40%.³⁹ Because the measured IC_{50} value was 19 μM , it can be seen that the inhibition was caused by the investigated compound and not by DMSO.

In the microplate assay, 10 μL of the enzyme preparation was preincubated with 460 μL of 0.1 M sodium–potassium phosphate buffer (pH 7.0) and 5 μL of a solution of the compound dissolved in DMSO and diluted with 0.1 M sodium–potassium phosphate buffer at 30 °C for 30 min. The controls contained 10 μL of enzyme preparation and 465 μL of 0.1 M sodium–potassium phosphate buffer (pH 7.0). The reaction was initiated by adding 25 μL of 4 mM Suc-Gly-Pro-7-amido-4-methylcoumarin dissolved in 0.1 M sodium–potassium phosphate buffer (pH 7.0), and the mixture was incubated at 30 °C for 60 min. The reaction was terminated by adding 500 μL of 1 M sodium acetate buffer (pH 4.2).

The formation of 7-amido-4-methylcoumarin was determined fluorometrically with microplate fluorescence reader (excitation at 360 nm and emission at 460 nm). The final concentration of the compounds in the assay mixture varied from 10^{-12} to 10^{-4} M.

The inhibitory activities (percent of control) were plotted against the log concentration of the compound, and the IC_{50} value was determined by nonlinear regression utilizing Graph-Pad Prism 3.0 software.

Molecular Modeling. Unless noted otherwise, molecular modeling was performed using Sybyl 6.9.0 and 6.9.1⁴⁰ with default options. To prepare the enzyme structure, the POP structure was derived from PDB (ID code 1QFS, resolution 2.0 Å). Prior to docking, the cocrystallized inhibitor was removed from the structure, and the hydrogen atoms were added using Sybyl Biopolymer module. Because the X-ray structure may also contain energetic tensions, an energetically favorable conformation of the suggested active site was searched by carrying out a molecular mechanics minimization using the MMFF94⁴¹ force field. Nitrogen NE2 of histidine 680 was not protonated while ND1 was protonated thus allowing interaction with ASP641.

The inhibitor structures (total number 52) were created using automatic translation from in-house ISIS database to mol2-files, using CONCORD⁴² software. After that, it was verified that the inhibitors had right configurations. The resulting structures were minimized using the MMFF94S force field as implemented in Sybyl. The following structures were docked into the active site of POP model using the GOLD^{28,43} program, version 2.2, with standard default settings unless otherwise mentioned. The docking area was defined using NE atom of ARG643 as a center, with a radius of 20 Å. Unfortunately, current docking programs cannot automatically take into account a possible covalent interaction between a ligand and a host. Because several of the compounds possibly have a covalent interaction, two violations for steric clashes were allowed. The docking procedure was repeated 10 times for each inhibitor using default parameters. All dockings, except for compound **32**, were ranked using GOLD score, and the best alternatives were visually inspected. For compound **32**, a CSCORE calculation within Sybyl was carried out.

The selected docking modes were further analyzed using the CoMSIA method. The CoMSIA descriptor fields (steric, electrostatic, hydrophobic, acceptor, donor) were calculated in a 3D cubic box extending 4 Å beyond the aligned inhibitors. Atomic point charges for inhibitors were calculated using the Gasteiger–Hückel model as implemented in Sybyl. pIC_{50} values were used as dependent variables in the PLS statistical analysis of the resulting data. The predictive value of the PLS model and the optimum number of the PLS components were evaluated by the progressive scrambling method.²⁹ The final noncross-validated model was developed using the optimal number of components that had both the highest scrambled q^2 value and the smallest value of the estimated cross-validated standard error with the slope of q^2 under 1.1.

Acknowledgment. We thank Tiina Koivunen, Jaana Leskinen, and Päivi Sutinen for their excellent technical assistance and Dr. Seppo Auriola and Unni Tengvall (M.Sc.) for performing the ESI-MS analyses. We also thank the National Technology Agency in Finland, Orion Pharma Oy, and the Finnish Cultural Foundation of Northern Savo for financial support.

Supporting Information Available: Elemental analyses of the end products and ¹H NMR data for the intermediate products. This material is available free of charge via the Internet at <http://pubs.acs.org>.

References

- (1) Barrett, A. J.; Rawlings, N. D. Oligopeptidases, and the emergence of the prolyl oligopeptidase family. *Biol. Chem. Hoppe Seyler* **1992**, *373*, 353–360.
- (2) O'Leary, R. M.; O'Connor, B. Identification and localisation of a synaptosomal membrane prolyl endopeptidase from bovine brain. *Eur. J. Biochem.* **1995**, *227*, 277–283.
- (3) Vanhoof, G.; Goossens, F.; Hendriks, L.; De Meester, I.; Hendriks, D.; Vriend, G.; Van Broeckhoven, C.; Scharpé, S. Cloning and sequence analysis of the gene encoding human lymphocyte prolyl endopeptidase. *Gene* **1994**, *149*, 363–366.
- (4) Koida, M.; Walter, R. Post-proline cleaving enzyme. Purification of this endopeptidase by affinity chromatography. *J. Biol. Chem.* **1976**, *251*, 7593–7599.
- (5) Huston, J. P.; Hasenöhrl, R. U. The role of neuropeptides in learning: Focus on the neurokinin substance P. *Behav. Brain Res.* **1995**, *66*, 117–127.
- (6) Dietrich, A.; Allen, J. D. Vasopressin and memory. I. The vasopressin analogue AVP4–9 enhances working memory as well as reference memory in the radial arm maze. *Behav. Brain Res.* **1997**, *87*, 195–200.
- (7) de Wied, D.; Gaffori, O.; van Ree, J. M.; de Jong, W. Central target for the behavioural effects of vasopressin neuropeptides. *Nature* **1984**, *308*, 276–278.
- (8) Dietrich, A.; Allen, J. D. Vasopressin and memory. II. Lesions to the hippocampus block the memory enhancing effects of AVP4–9 in the radial maze. *Behav. Brain Res.* **1997**, *87*, 201–208.
- (9) Miyamoto, M.; Hirai, K.; Takahashi, H.; Kato, K.; Nishiyama, M.; Okada, H.; Nagaoka, A. Effects of sustained release formulation of thyrotropin-releasing hormone on learning impairments caused by scopolamine and AF64A in rodents. *Eur. J. Pharmacol.* **1993**, *238*, 181–189.
- (10) Yankner, B. A.; Duffy, L. K.; Kirschner, D. A. Neurotrophic and neurotoxic effects of amyloid beta protein: Reversal by tachykinin neuropeptides. *Science* **1990**, *250*, 279–282.
- (11) Irazusta, J.; Larrinaga, G.; Gonzalez-Maeso, J.; Gil, J.; Meana, J. J.; Casis, L. Distribution of prolyl endopeptidase activities in rat and human brain. *Neurochem. Int.* **2002**, *40*, 337–345.
- (12) Kato, T.; Okada, M.; Nagatsu, T. Distribution of post-proline cleaving enzyme in human brain and the peripheral tissues. *Mol. Cell. Biochem.* **1980**, *32*, 117–121.
- (13) Bellemere, G.; Vaudry, H.; Mounien, L.; Boutelet, I.; Jegou, S. Localization of the mRNA encoding prolyl endopeptidase in the rat brain and pituitary. *J. Comput. Neurol.* **2004**, *471*, 128–143.
- (14) Jiang, C. H.; Tsien, J. Z.; Schultz, P. G.; Hu, Y. The effects of aging on gene expression in the hypothalamus and cortex of mice. *Proc. Natl. Acad. Sci. U.S.A.* **2001**, *98*, 1930–1934.
- (15) Rampon, C.; Jiang, C. H.; Dong, H.; Tang, Y. P.; Lockhart, D. J.; Schultz, P. G.; Tsien, J. Z.; Hu, Y. Effects of environmental enrichment on gene expression in the brain. *Proc. Natl. Acad. Sci. U.S.A.* **2000**, *97*, 12880–12884.
- (16) Shishido, Y.; Furushiro, M.; Tanabe, S.; Nishiyama, S.; Hashimoto, S.; Ohno, M.; Yamamoto, T.; Watanabe, S. ZTTA, a postproline cleaving enzyme inhibitor, improves cerebral ischemia-induced deficits in a three-panel runway task in rats. *Pharmacol. Biochem. Behav.* **1996**, *55*, 333–338.
- (17) Shishido, Y.; Furushiro, M.; Tanabe, S.; Taniguchi, A.; Hashimoto, S.; Yokokura, T.; Shibata, S.; Yamamoto, T.; Watanabe, S. Effect of ZTTA, a prolyl endopeptidase inhibitor, on memory impairment in a passive avoidance test of rats with basal forebrain lesions. *Pharm. Res.* **1998**, *15*, 1907–1910.
- (18) Yoshimoto, T.; Kado, K.; Matsubara, F.; Koriyama, N.; Kaneto, H.; Tsuru, D. Specific inhibitors for prolyl endopeptidase and their anti-amnesic effect. *J. Pharmacobiodyn.* **1987**, *10*, 730–735.
- (19) Schneider, J. S.; Giardiniere, M.; Morain, P. Effects of the prolyl endopeptidase inhibitor S 17092 on cognitive deficits in chronic low dose MPTP-treated monkeys. *Neuropsychopharmacology* **2002**, *26*, 176–182.

- (20) Grellier, P.; Vendeville, S.; Joyeau, R.; Bastos, I. M.; Drobecq, H.; Frappier, F.; Teixeira, A. R.; Schrével, J.; Davioud-Charvet, E.; Sergheraert, C.; Santana, J. M. *Trypanosoma cruzi* prolyl oligopeptidase Tc80 is involved in nonphagocytic mammalian cell invasion by trypomastigotes. *J. Biol. Chem.* **2001**, *276*, 47078–47086.
- (21) Wallén, E. A. A.; Christiaans, J. A. M.; Forsberg, M. M.; Venäläinen, J. I.; Männistö, P. T.; Gynther, J. Dicarboxylic acid bis(L-prolyl-pyrrolidine) amides as prolyl oligopeptidase inhibitors. *J. Med. Chem.* **2002**, *45*, 4581–4584.
- (22) Wallén, E. A. A.; Christiaans, J. A. M.; Jarho, E. M.; Forsberg, M. M.; Venäläinen, J. I.; Männistö, P. T.; Gynther, J. New prolyl oligopeptidase inhibitors developed from dicarboxylic acid bis-(L-prolyl-pyrrolidine) amides. *J. Med. Chem.* **2003**, *46*, 4543–4551.
- (23) Klebe, G.; Abraham, U.; Mietzner, T. Molecular similarity indices in a comparative analysis (CoMSIA) of drug molecules to correlate and predict their biological activity. *J. Med. Chem.* **1994**, *37*, 4130–4146.
- (24) Wallén, E. A. A.; Christiaans, J. A. M.; Saarinen, T. J.; Jarho, E. M.; Forsberg, M. M.; Venäläinen, J. I.; Männistö, P. T.; Gynther, J. Conformationally rigid N-acyl-5-alkyl-L-prolyl-pyrrolidines as prolyl oligopeptidase inhibitors. *Bioorg. Med. Chem.* **2003**, *11*, 3611–3619.
- (25) Wallén, E. A. A.; Christiaans, J. A. M.; Saario, S. M.; Forsberg, M. M.; Venäläinen, J. I.; Paso, H. M.; Männistö, P. T.; Gynther, J. 4-Phenylbutanoyl-2(S)-acylpyrrolidines and 4-phenylbutanoyl-L-prolyl-2(S)-acylpyrrolidines as prolyl oligopeptidase inhibitors. *Bioorg. Med. Chem.* **2002**, *10*, 2199–2206.
- (26) Jarho, E. M.; Venäläinen, J. I.; Huuskonen, J.; Christiaans, J. A. M.; Garcia-Horsman, J. A.; Forsberg, M. M.; Järvinen, T.; Gynther, J.; Männistö, P. T.; Wallén, E. A. A. A cyclopent-2-enecarbonyl group mimics proline at the P2 position of prolyl oligopeptidase inhibitors. *J. Med. Chem.* **2004**, *47*, 5605–5607.
- (27) Fülöp, V.; Böcskei, Z.; Polgár, L. Prolyl oligopeptidase: An unusual beta-propeller domain regulates proteolysis. *Cell* **1998**, *94*, 161–170.
- (28) Jones, G.; Willett, P.; Glen, R. C.; Leach, A. R.; Taylor, R. Development and validation of a genetic algorithm for flexible docking. *J. Mol. Biol.* **1997**, *267*, 727–748.
- (29) Clark, R. D.; Fox, P. C. Statistical variation in progressive scrambling. *J. Comput.-Aided Mol. Des.* **2004**, *18*, 563–576.
- (30) Arai, H.; Nishioka, H.; Niwa, S.; Yamanaka, T.; Tanaka, Y.; Yoshinaga, K.; Kobayashi, N.; Miura, N.; Ikeda, Y. Synthesis of prolyl endopeptidase inhibitors and evaluation of their structure–activity relationships: In vitro inhibition of prolyl endopeptidase from canine brain. *Chem. Pharm. Bull.* **1993**, *41*, 1583–1588.
- (31) Portevin, B.; Benoist, A.; Rémond, G.; Hervé, Y.; Vincent, M.; Lepagnol, J.; De Nanteuil, G. New prolyl endopeptidase inhibitors: in vitro and in vivo activities of azabicyclo[2.2.2]octane, azabicyclo[2.2.1]heptane, and perhydroindole derivatives. *J. Med. Chem.* **1996**, *39*, 2379–2391.
- (32) Yoshimoto, T.; Tsuru, D.; Yamamoto, N.; Ikezawa, R.; Furukawa, S. Structure activity relationship of inhibitors specific for prolyl endopeptidase. *Agric. Biol. Chem.* **1991**, *55*, 37–43.
- (33) Toide, K.; Iwamoto, Y.; Fujiwara, T.; Abe, H. JTP-4819: A novel prolyl endopeptidase inhibitor with potential as a cognitive enhancer. *J. Pharmacol. Exp. Ther.* **1995**, *274*, 1370–1378.
- (34) Wilk, S.; Orłowski, M. Inhibition of rabbit brain prolyl endopeptidase by n-benzyloxycarbonyl-prolyl-prolinal, a transition state aldehyde inhibitor. *J. Neurochem.* **1983**, *41*, 69–75.
- (35) Tanaka, Y.; Niwa, S.; Nishioka, H.; Yamanaka, T.; Torizuka, M.; Yoshinaga, K.; Kobayashi, N.; Ikeda, Y.; Arai, H. New potent prolyl endopeptidase inhibitors: synthesis and structure–activity relationships of indan and tetralin derivatives and their analogues. *J. Med. Chem.* **1994**, *37*, 2071–2078.
- (36) Liang, T. C.; Abeles, R. H. Inhibition of papain by nitriles: mechanistic studies using NMR and kinetic measurements. *Arch. Biochem. Biophys.* **1987**, *252*, 626–634.
- (37) Brisson, J. R.; Carey, P. R.; Storer, A. C. Benzoylamidoacetone nitrile is bound as a thioimidate in the active site of papain. *J. Biol. Chem.* **1986**, *261*, 9087–9089.
- (38) Venäläinen, J. I.; Juvonen, R. O.; Garcia-Horsman, J. A.; Wallén, E. A. A.; Christiaans, J. A. M.; Jarho, E. M.; Gynther, J.; Männistö, P. T. Slow-binding inhibitors of prolyl oligopeptidase with different functional groups at the P1 site. *Biochem. J.* **2004**, *382*, 1003–1008.
- (39) Venäläinen, J. I.; Juvonen, R. O.; Forsberg, M. M.; Garcia-Horsman, J. A.; Poso, A.; Wallén, E. A. A.; Gynther, J.; Männistö, P. T. Substrate-dependent, nonhyperbolic kinetics of pig brain prolyl oligopeptidase and its tight binding inhibition by JTP-4819. *Biochem. Pharmacol.* **2002**, *64*, 463–471.
- (40) Tripos Inc. SYBYL; S. H. R.: St. Louis, MO.
- (41) Halgren, T. Maximally diagonal force constants in dependent angle-bending coordinates. 2. Implications for the design of empirical force fields. *J. Am. Chem. Soc.* **1990**, *112*, 4710–4723.
- (42) Pearlman, R. S. *Concord User's Manual*; Distributed by Tripos Inc.: St. Louis, MO, 2004.
- (43) Jones, G.; Willett, P.; Glen, R. C. Molecular recognition of receptor sites using a genetic algorithm with a description of desolvation. *J. Mol. Biol.* **1995**, *245*, 43–53.

JM0500020